

PACS numbers: 42.55.Vc; 52.50.Jm
DOI: 10.1070/QE2009v039n09ABEH014069

Simulation of an X-ray laser in the transient gain-saturation regime*

F.A. Starikov, V.A. Volkov, P.D. Gasparyan, V.I. Roslov

***Abstract*. By using the TRANS code, we performed three-dimensional calculations of amplified spontaneous emission (ASE) in X-ray lasers on the 3p – 3s transition in Ne-like Ge ($\lambda = 19.6$ nm) and Ti ($\lambda = 2.6$ nm) operating in the transient regime upon irradiation of a flat target by a high-power picosecond laser pulse focused into a line with one or two nanosecond prepulses. The hydrodynamics and population kinetics of the active medium of X-ray lasers were calculated by using the SS-9M code. The pulse duration, the gain, the spatial structure of the laser beam and the type of influence of a 'travelling' pump wave on the ASE brightness obtained in calculations are in agreement with the experimental data. The use of the 'travelling pump wave' leads not only to the increase in the ASE brightness but also considerably reduces its angular divergence.**

Keywords: *X-ray laser, amplified spontaneous emission, 'travelling pump wave', three-dimensional calculation.*

1. Introduction

One of the methods of producing the hot plasma of multiply charged ions as the active medium for an X-ray laser is the focusing of high-power optical laser radiation into a line on the surface of a solid target [1]. X-rays are generated in the produced extended plasma column in the amplified spontaneous emission (ASE) regime. The most popular are schemes based on the collision pumping of Ne- and Ni-like ions, where an electron is excited to the upper laser level from the ground state in collisions with free electrons. Along with increasing the energy and decreasing the emission wavelength of an X-ray laser, of current interest is also the problem of the ASE beam quality [2] because many applications of X-ray lasers depend on it.

The aim of the simulation of an X-ray laser is to find the optimal conditions for the generation and formation of ASE beams. The TRANS computer code [3, 4] is intended for the three-dimensional nonsteady-state calculation of ASE in the X-ray laser taking into account amplification, absorption, diffraction, refraction, and scattering of X-rays in plasma. As the input parameters, the TRANS code uses the spatiotemporal distributions of plasma parameters obtained preliminarily in the calculations of the plasma hydrodynamics and the population kinetics in the plasma.

Upon pumping by a nanosecond laser pulse, the quasi-steady-state amplification regime is realised in an X-ray laser. In this case, transient processes related to the finite transverse relaxation (collision dephasing) time can be neglected [2]. The three-dimensional TRANS calculations of the ASE dynamics for the X-ray laser on the 19.6-nm 3p – 3s transition in the Ne-like ion Ge [5, 6] realised on the Iskra-5 facility at the Russian Federal Nuclear Center – VNIIEF are in good agreement with experimental data on the far-field ASE brightness distribution and the gain [7 – 10].

If the X-ray laser uses pumping of the preliminarily prepared plasma by a high-power picosecond laser, the population inversion is produced in transient collision processes proceeding at different rates [11]. The transient amplification regime provides the gain of a few tens of inverse centimetres and ensures a higher ASE peak power compared to the quasi-steady-state regime. In this case, the physical model becomes more complicated, which hinders adequate three-dimensional simulations. For example, the COLAX code developed in France for calculating the ASE dynamics in X-ray lasers is two-dimensional [12, 13].

The aim of this work is to obtain, by using three-dimensional TRANS simulations, the spatiotemporal parameters of the ASE beam in an X-ray laser operating in the transient regime. Such simulations were performed earlier in the linear gain approximation for an X-ray laser operating on the Ne-like Ti ion [7, 8]. However, the linear gain approximation may not be fulfilled for the gain α of a few tens of inverse centimetres and the X-ray laser length $L \sim 1$ cm because the gain saturation begins to play a noticeable role for $\alpha L \sim 15 - 20$ (at least, in the quasi-steady-state regime) [1, 2]. In this work, we use the updated TRANS code to solve the equations of the ASE dynamics, polarisation of the medium at the laser transition and populations of the upper (N_u) and lower (N_l) laser levels taking into account stimulated radiation. The spatiotemporal distribution of the medium parameters by neglecting radiation transfer at the laser transition is taken from calculations by using the SS-9M code [14]. The ASE parameters were calculated for an X-ray laser on Ne-like Ge and Ti ions. The calculated parameters of the X-ray laser are compared with experimental data.

* Reported at the Conference 'Laser Optics 2008', St. Petersburg, Russia.

F.A. Starikov, V.A. Volkov, P.D. Gasparyan, V.I. Roslov Russian Federal Nuclear Center, All-Russian Research Institute of Experimental Physics, prosp. Mira 37, 607190 Sarov, Nizhnii Novgorod region, Russia; e-mail: fstar@rol.ru

Received 11 February 2009
Kvantovaya Elektronika **39** (9) 825 – 829 (2009)
Translated by M.N. Sapozhnikov

2. Theoretical model

The theoretical model and TRANS code [3, 4, 7, 8] describing transient ASE in an extended plasma medium are based on the semi-classical system of equations

$$\left[\pm\frac{\partial}{\partial z}+\frac{1}{c}\frac{\partial}{\partial t}+\frac{\mathrm{i}}{2k}\nabla_\perp^2+\frac{\mathrm{i}k}{2}(\varepsilon-1)+\frac{\beta}{2}\right]A_\pm=\frac{k}{2\mathrm{i}}p_\pm, \quad (1)$$

$$\left(\frac{\partial}{\partial t}+\frac{1}{\tau_2}-\mathrm{i}\Delta\omega\right)p_\pm=\frac{\mathrm{i}\alpha}{k\tau_2}A_\pm+S_\pm, \quad (2)$$

where A_+ and A_- are the complex field amplitudes of two ASE fluxes propagating in the opposite directions; p_+ and p_- are the complex amplitudes of the polarisation of a medium at the laser transition; S_+ and S_- are stochastic polarisation sources in the medium volume (Langevin forces); $\nabla_\perp^2$ is the Laplacian over the transverse coordinate $\boldsymbol{r}=\boldsymbol{i}x+\boldsymbol{j}y$; z is the longitudinal coordinate; $k=\omega/c$ is the wave number; ε is the permittivity ($\varepsilon\approx 1$); β is the nonresonance absorption coefficient; $\Delta\omega=\omega-\omega_0$; ω is the carrier radiation frequency; and ω_0 is the laser transition frequency.

The transverse relaxation time τ_2 describes radiative and collision processes resulting in the broadening of a Lorentzian spectral line. The inhomogeneous broadening mechanisms (for example, Doppler effect) lead to the additional decay of polarisation. By neglecting the Lamb dips, the inhomogeneous broadening can be approximately taken into account within the Lorentzian contour, although the solution of a number of equations of type (2) with different frequency detunings would be a more correct approach. In this case, the right side of equations (1) will contain the sum of quantities p_+ and p_-, each of them having a weight corresponding to the spectral line profile at a given temperature. In this paper, we give most attention to spatial effects in the ASE dynamics, and $\omega=\omega_0$ in calculations, while frequency ω_0 is constant for all emitters.

The field amplitudes $A_\pm$ in (1) and (2) are normalised so that the ASE flux densities are $J_\pm=|A_\pm|^2$. The initial polarisations and spontaneous sources satisfy the correlation relations

$$\langle p_{\pm0}(\boldsymbol{r}_1,z_1)p_{\pm0}^*(\boldsymbol{r}_2,z_2)\rangle=\left(4j_\mathrm{s}/k^2\right)F_\mathrm{s}(\boldsymbol{r}_1-\boldsymbol{r}_2)\delta(z_1-z_2), \quad (3)$$

$$\langle S_\pm(\boldsymbol{r}_1,z_1,t_1)S_\pm^*(\boldsymbol{r}_2,z_2,t_2)\rangle=\left[8j_\mathrm{s}/\left(k^2\tau_2\right)\right]$$

$$\times F_\mathrm{s}(\boldsymbol{r}_1-\boldsymbol{r}_2)\delta(z_1-z_2)\delta(t_1-t_2), \quad (4)$$

where j_s is the spontaneous noise intensity (in W st^{-1} cm^{-3}); $F_\mathrm{s}(\boldsymbol{r}_1-\boldsymbol{r}_2)$ is the transverse correlation function determining the unit intensity of spontaneous emission within the solid angle θ_s, which exceeds in calculations the angular width of the transmission band of the system.

Information on the electron and ion temperatures, the charge composition, the ion and electron concentrations, etc. is preliminarily found from hydrodynamic and kinetic SS-9M calculations of the laser plasma. The kinetic model in the balance approximation, which is based on the solution of a system of nonsteady-state equations for populations of discrete ion states, takes into account all significant radiative–collision processes in plasma. The fine splitting of the excited levels of Ne-like ions with the principal quantum number $n\leqslant 4$ is taken into account. The calculations give the spatiotemporal distributions of the electron density N_e (and, correspondingly, the permittivity $\varepsilon=1-N_\mathrm{e}/N_\mathrm{c}$ where N_c is the critical plasma density), the nonresonance absorption coefficient β, the gain cross section σ for $\omega=\omega_0$, and the populations of the upper (N_ur0) and lower (N_lr0) laser levels taking into account pumping and kinetic relaxation and neglecting radiation transfer at the laser transition. The small-signal gain (in the absence of stimulated emission) is $\alpha_0=\sigma\Delta N_\mathrm{r0}$, where $\Delta N_\mathrm{r0}=N_\mathrm{ur0}-g_\mathrm{u}N_\mathrm{lr0}/g_\mathrm{l}$ is the population inversion and g_u and g_l are the statistical weights of the upper and lower laser levels.

In the linear gain approximation, when the ASE intensity in the medium is considerably lower than the saturation intensity [2], equations (1) and (2) were integrated with the found distribution of the small-signal gain $\alpha=\alpha_0$ [7, 8]. In this paper, we solved simultaneously equations (1) and (2) and equations for populations of the upper and lower laser levels taking into account stimulated emission:

$$\frac{\partial N_\mathrm{u}}{\partial t}=\frac{\partial N_\mathrm{ur0}}{\partial t}-\frac{1}{\hbar c}\,\mathrm{Im}(A_+^*p_++A_-^*p_-), \quad (5)$$

$$\frac{\partial N_\mathrm{l}}{\partial t}=\frac{\partial N_\mathrm{lr0}}{\partial t}+\frac{1}{\hbar c}\,\mathrm{Im}(A_+^*p_++A_-^*p_-). \quad (6)$$

Thus, equations for N_u and N_l are solved by the splitting method in two stages: first, their slower variation, related to pumping and kinetic relaxation, is taken into account in the SS-9M code and then stimulated emission is taken into account in the TRANS code. From (5) and (6), the gain $\alpha=\sigma\Delta N=\sigma(N_\mathrm{u}-g_\mathrm{u}N_\mathrm{l}/g_\mathrm{l})$ is found to be substituted into (2) and the spontaneous noise intensity $j_\mathrm{s}=\hbar\omega A_\mathrm{ul}N_\mathrm{u}/(4\pi)$, where A_ul is the probability of the spontaneous radiative transition between laser levels.

3. Results of calculations for the Ne-like Ge ion X-ray laser

The scheme of the X-ray laser is shown in Fig. 1a. Optical radiation from a pump laser focused to a line is incident on a flat target. During irradiation of the target, a plasma column is produced along the z axis, which is expanding in the transverse direction. The width of the irradiation line is 50 μm.

Figure 1b shows schematically the time distribution of the 1.06-μm pump radiation intensity for a 19.6-nm X-ray laser on the 3p–3s transition of the Ne-like Ge ion, which is

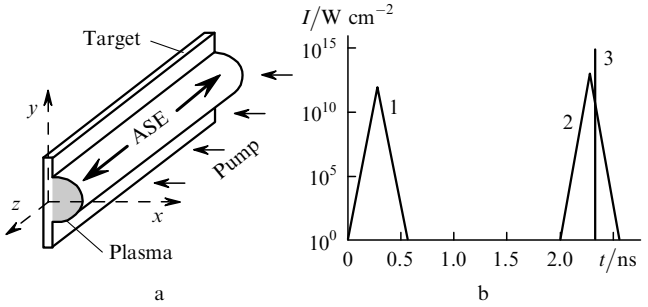

Figure 1. Scheme of the X-ray laser (a) and the time dependence of the pump intensity (b).

close to that presented in [15]. All the pump pulses have a triangular shape. First a Ge target is irradiated by 10^{12}-W cm^{-2} prepulse 1 with a base duration of 0.56 ns. This prepulse produces a plasma column with the abundance of Ne-like Ge ions. Within 2 ns after relaxation of the plasma column and a decrease in the transverse gradient of the electron density, higher-power 10^{13}-W cm^{-2}, 0.56-ns pump pulse 2 is incident on the target.

Pulse 2 heats the plasma and produces the population inversion. During irradiation of the target by this pulse, additional 10^{15}-W cm^{-1}, 3.4-ps pulse 3, delayed by 2.33 ns with respect to pulse 1, is incident on the target. This pumping scheme differs from the quasi-steady-state scheme in [5–10] by the presence of high-power pulse 3.

Figure 2 shows the distributions of the small-signal gain $\alpha_0 = \sigma\Delta N_{r0}$ at the strongest $3p\,(J=0) - 3s\,(J=1)$ transition and of the electron density N_e calculated by using the SS-9M code. Amplification in the X-ray laser begins to develop during the action of pump pulse 2. The gain α_0 is a few inverse centimetres, which is typical for the quasi-steady-state regime [1, 2]. After the action of high-power pump pulse 3 at the instant $t \approx 2.33$ ns, α_0 drastically increases up to 40 cm^{-1}. This means that amplification is realised in the transient regime. Then, after the action of pump pulse 3, the gain drastically decreases, but does not vanish. Because pump pulse 2 still acts, the conditions for quasi-steady-state amplification are preserved.

The spatiotemporal parameters of the ASE beam at the X-ray laser output and in the far-field zone were obtained in three-dimensional TRANS calculations. It was assumed that the target was irradiated in the 'travelling wave' regime. The ASE power dynamics at both ends of the X-ray laser is shown in Fig. 3. For the X-ray laser length $L = 3$ mm, the quasi-steady-state signal gives a noticeable contribution to the total X-ray laser energy, its contribution decreasing with increasing L. The use of the 'travelling pump wave' is especially important with increasing the X-ray laser length, when the laser emits virtually in one direction. The output ASE pulse duration is ~ 10 ps, exceeding the duration of pump pulse 3 by several times. Such an elongation of the ASE pulse caused by transient processes, which is also observed during linear amplification [7, 8], agrees with experimental data [16].

Figure 4 shows time-integrated far-field ASE intensity distributions. For $L = 3$ mm, the ASE brightness has the bell-shaped distribution and acquires strongly modulated speckle pattern with increasing L. For $L = 3$ mm, the contribution of the quasi-steady-state signal to the ASE energy is significant, while its duration considerably exceeds the ASE coherence time. As a result, the spatial speckle pattern is 'smeared' during the action of the ASE pulse. For $L = 6$ mm, the total signal is mainly determined by transient ASE with a small pulse duration comparable with its coherence time, while time averaging does not virtually occur. The measurements of the coherence time [17] and the spatial structure of the ASE beam [18] confirm these calculations.

The ASE beam is deflected to the side from the target

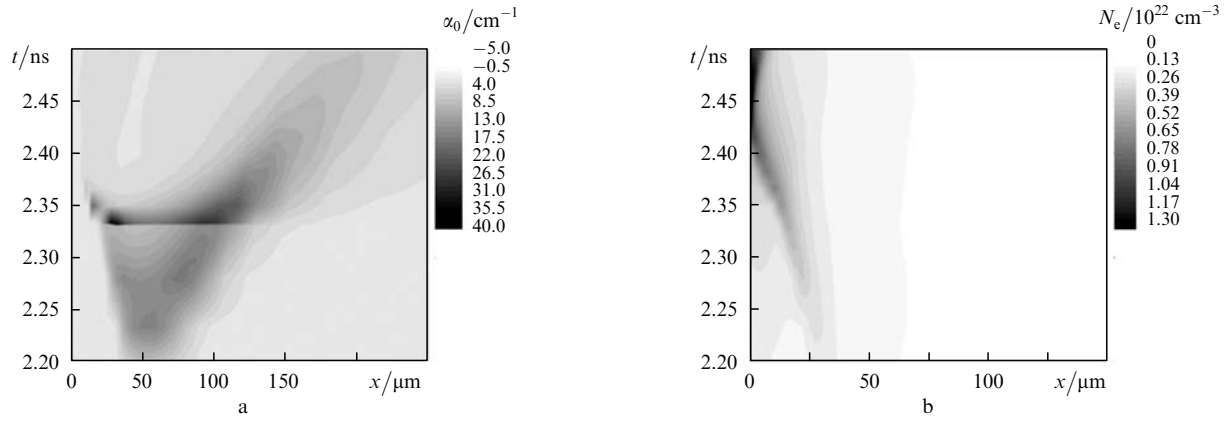

Figure 2. Spatiotemporal distributions of the small-signal gain α_0 (a) and electron density N_e (b) in the Ne-like Ge ion X-ray laser.

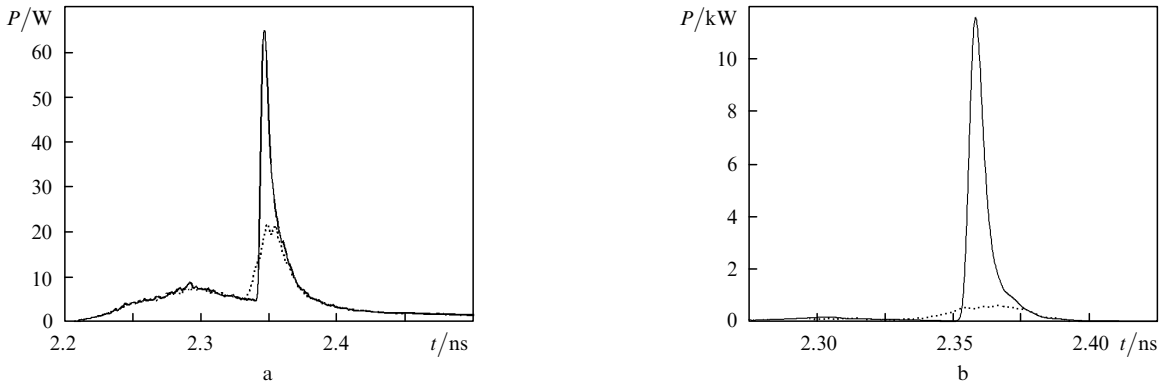

Figure 3. ASE power dynamics in the 'travelling pump wave' direction (solid curves) and in the opposite direction (dashed curves) for the Ne-like Ge ion X-ray laser for $L = 3$ (a) and 6 mm (b).

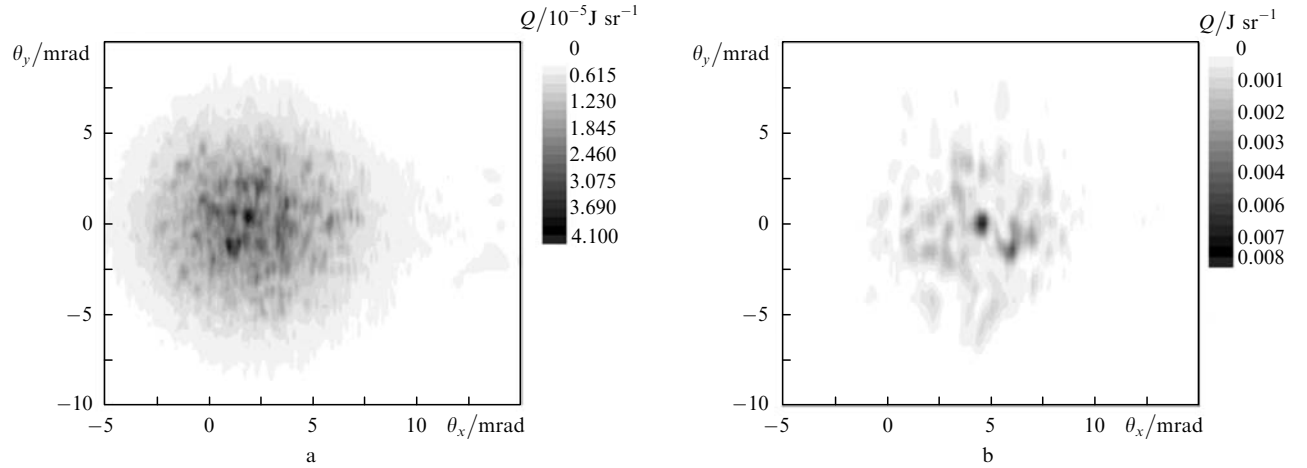

Figure 4. Far-field ASE brightness distribution for the Ne-like Ge ion X-ray laser for $L = 3$ (a) and 6 mm (b).

due to refraction, this deflection being ~ 5 mrad for $L =$ 6 mm. The angular divergence of ASE along the x axis is 5–10 mrad. The ASE beam is multimode, the radius of the transverse spatial coherence of ASE being approximately an order of magnitude lower than the beam radius.

4. Results of calculations for the Ne-like Ti ion X-ray laser

The hydrodynamics and kinetics of the active medium of the 32.6-nm X-ray laser on the 3p–3s transition of the Ne-like Ti ion were calculated by using the SS-9M code for conditions typical for experiments with the Sokol-P laser facility at the RFNC–VNIITF [19, 20]. The width of the irradiation line alone the y axis was 40 μm (Fig. 1a).

The time distribution of the pump intensity is similar to that shown in Fig. 1b, except the absence of pulse 2. The target is first irradiated by 6×10^{11} W cm^{-2} triangle prepulse 1 with a FWHM of 0.42 ns. Then, main 4-ps, 2.5×10^{14} W cm^{-2} pulse 3 follows with a delay of 1.48 ns.

Figure 5a shows the distribution of the gain α_0 at the $3p\,(J = 0) - 3s\,(J = 1)$ transition, which achieves 130 cm^{-1} in maximum. Figure 5b presents the dependence of the maximum average ASE brightness in the far-field zone on the length L in the absence of the 'travelling pump wave. The brightness increases with increasing L and tends to a constant value. Also, a curve is presented which is obtained by neglecting the gain saturation [neglecting the contribution of stimulated emission in equations (5) and (6)]. One can see that the influence of the gain saturation begins for $L > 3$ mm, in accordance with experiments [19, 20]. Although the peak value of α_0 are huge, the observed gain for $L < 3$ mm is 30–35 cm^{-1}, which is close to the experimental value [19, 20]. Figure 5b shows that the use of the 'travelling pump wave' provides the increase in the ASE brightness by an order of magnitude (in experiments [20] for $L = 8$ mm, approximately the five-fold increase in the brightness was observed).

The time-integrated far-field ASE brightness distributions for $L = 8$ mm in the absence and presence of the 'travelling pump wave' are shown in Fig. 6. As in the case of the Ne-like Ge ion, ASE is spatially incoherent, but the use of the 'travelling pump wave' leads to a considerable decrease in the angular divergence of ASE.

5. Conclusions

By using the TRANS code, we have performed three-dimensional calculations of ASE in the X-ray laser on the $3p\,(J = 0) - 3s\,(J = 1)$ transition in Ne-like Ge and Ti ions.

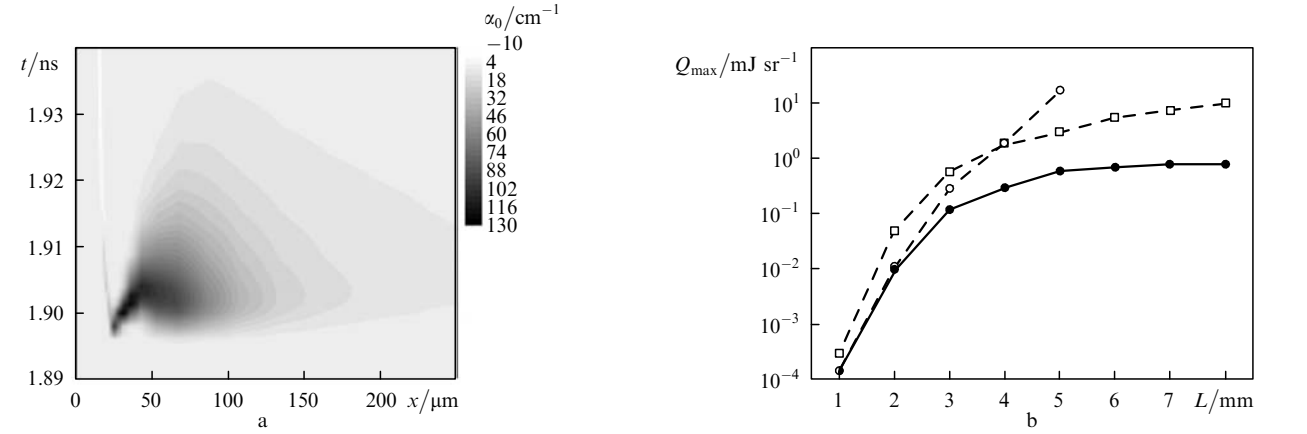

Figure 5. Spatiotemporal distribution of the small-signal gain α_0 in the Ne-like Ti ion X-ray laser (a) and dependences of the ASE brightness Q_{max} of the X-ray laser length in the absence (●) and presence (□) of the 'travelling pump wave' and in the absence of the 'travelling pump wave' by neglecting the gain saturation (○) (b).

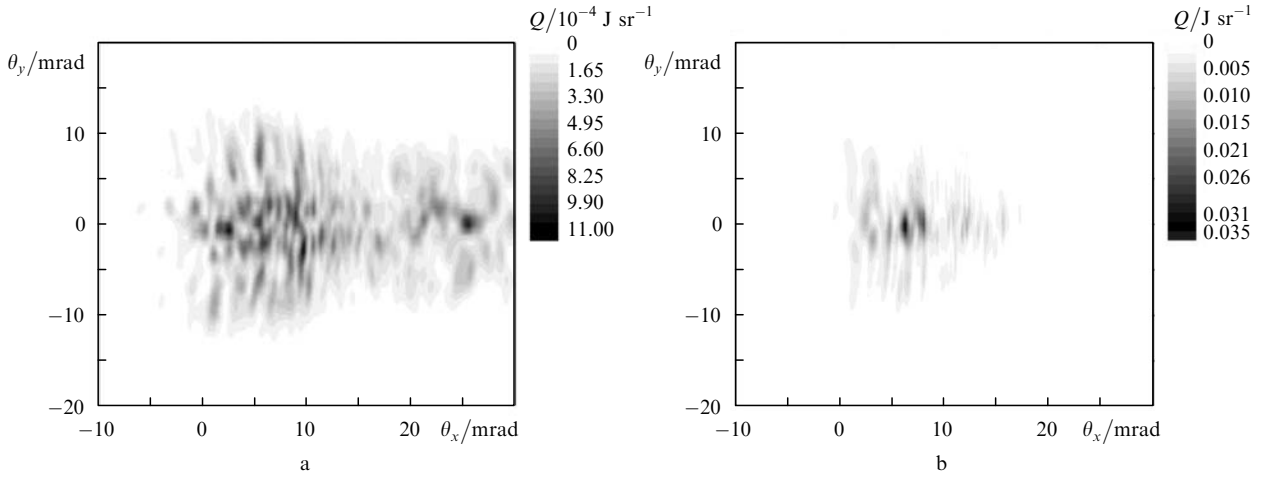

Figure 6. Far-field ASE brightness distributions for $L = 8$ mm in the absence (a) and presence (b) of the 'travelling pump wave' in the Ne-like Ti ion X-ray laser.

The plasma active medium of the X-ray laser is produced by focusing radiation from an optical laser to a line on a flat target. The pump scheme uses one or two nanosecond prepulses and a high-power picosecond pulse to obtain amplification in the transient regime. The hydrodynamics and kinetics of the population of ion levels in the plasma was calculated by using the SS-9M code. We have calculated the spatiotemporal parameters of the ASE beam, which are consistent with experimental data. The ASE pulse duration exceeds the duration of the picosecond pump pulse, the ASE beam has the multimode speckled structure, and the observed gain is considerable lower than its peak values. The use of the 'travelling pump wave' provides not only the increase in the ASE brightness but also considerably reduces the angular ASE divergence. Our calculations have confirmed that the TRANS code can be a reliable tool for finding the optimal operation conditions for X-ray lasers and generating high-quality ASE beams.

References

1. Elton R.C. *X-ray Lasers* (San Diego: Acad. Press, 1991; Moscow: Mir, 1994).
2. Gasparyan P.D., Starikov F.A., Starostin A.N. *Usp. Fiz. Nauk*, **168**, 843 (1998) [*Phys. Uspekhi*, **41** 761 (1998)].
3. Starikov F.A., Gasparyan P.D., Ladagin V.K., in *Annotatsii Mezhdunarodnoi konferentsii 'IV Kharitonovskie nauchnye chteniya'* (Annotation of the International Conference on IV Khariton Scientific Readings) (Sarov, 2002) p. 82.
4. Starikov F.A., Gasparyan P.D., Ladagin V.K. *Tezisy dokladov XXX Zvenigorodskoi konferentsii po fizike plazmy i UTC* (Theses of Reports of the XXX Zvenigorod Conference on Plasma Physics and CTF) (Zvenigorod, 2003) (Moscow, 2003) p. 142.
5. Abzaev F.M., Aleksandrovich R.E., Annenkov V.I., et al., in *Annotatsii Mezhdunarodnoi konferentsii 'IV Kharitonovskie nauchnye chteniya'* (Annotations of the International Conference on IV Khariton Scientific Readings) (Sarov, 2002) p. 83.
6. Abzaev F.M., Aleksandrovich R.E., Annenkov V.I., et al. *Techn. Dig. Int. Quantum Electron. Conf. (IQEC'2002)* (Moscow, 2002) Paper QsuA3, p. 42.
7. Starikov F.A., Bessarab A.V., Gasparyan P.D., et al. *Proc. SPIE Int. Soc. Opt. Eng.*, **5197**, 60 (2003).
8. Starikov F.A., Bessarab A.V., Gasparyan P.D., et al. *Trudy RFNC-VNIIEF*, (9), 186 (2005).
9. Starikov F.A., Bessarab A.V., Gasparyan P.D., et al. *Proc. SPIE Int. Soc. Opt. Eng.*, **5777**, 623 (2005).
10. Starikov F.A., Abzaev F.M., Annenkov V.I., et al. *J. Phys. IV*, **133**, 1197 (2006).
11. Afanas'ev Yu.V., Shlyaptsev V.N. *Kvantovaya Elektron.*, **16**, 2499 (1989) [*Sov. J. Quantum Electron.*, **19**, 1606 (1989)].
12. Larroche O., Ros D., Klisnick A., et al. *Phys. Rev. A*, **62**, 043815 (2000).
13. Al'miev R., Larroche O., Benredjem D., et al. *Phys. Rev. Lett.*, **99**, 123902 (2007).
14. Voinov B.A., Gasparyan P.D., Kochubei Yu.K., Roslov V.I. *VANT, Ser. Met. Progr. Chisl. Resh. Zadach Mat. Fiz.*, No. 2, 65 (1993).
15. Lin J.Y., Tallents G.J., MacPhee A.G., et al. *Opt. Commun.*, **166**, 211 (1999).
16. Dunn J., Smith R.F., Shepherd R., et al. *Proc. SPIE Int. Soc. Opt. Eng.*, **5197**, 51 (2003).
17. Dunn J., Smith R.F., Hubert S., et al. *Proc. SPIE Int. Soc. Opt. Eng.*, **5197**, 43 (2003).
18. Nilsen J., Dunn J., Smith R.F. *Proc. SPIE Int. Soc. Opt. Eng.*, **5197**, 205 (2003).
19. Andriyash A.V., Vikhlyaev D.A., Gavrilov D.S., et al. *Kvantovaya Elektron.*, **36**, 511 (2006) [*Quantum Electron.*, **36**, 511 (2006)].
20. Andriyash A.V., Vikhlyaev D.A., Gavrilov D.S., et al., in *Tezisy Mezhdunarodnoi konferentsii 'X Kharitonovskie nauchnye chteniya'* (Theses of the International Conference on X Khariton Scientific Readings) (Sarov, 2002) pp 227 – 228.